

Zero-temperature properties of matter and the quantum theorem of corresponding states: The liquid-to-crystal phase transition for Fermi and Bose systems*

L. H. Nosanow, L. J. Parish, and F. J. Pinski

*School of Physics and Astronomy, University of Minnesota, Minneapolis, Minnesota 55455
and Department of Physics and Astronomy, University of Florida, Gainesville, Florida 32611*

(Received 1 July 1974)

The zero-temperature properties of matter with an interaction pair potential of the Lennard-Jones form are studied in the context of the quantum theorem of corresponding states. In particular, the phase transition between the fluid and crystalline phases is studied for systems obeying either Fermi-Dirac or Bose-Einstein statistics. It is found that the solidification pressure of a Fermi system is much lower than that of a Bose system with the same mass and pair potential. We find that it is illuminating to extend the usual thermodynamic variable space to include the corresponding-states quantum parameter $\eta \equiv h^2/m\epsilon\sigma^2$ which is defined in the text. It is shown that phase transitions occur at zero temperature as η is varied; in particular, a first-order liquid-solid transition is described in detail and a model is discussed in which a second-order magnetic transition occurs at a critical value of η . It is suggested that the full complexity of the phase-transition behavior, which is observed at finite temperatures arising from various properties of the potential, will also be observed at zero temperature mainly as a fundamental consequence of the quantum-mechanical zero-point kinetic energy.

I. INTRODUCTION

The quantum theorem of corresponding states (QTCS) was originally proposed and discussed by de Boer and co-workers.¹⁻³ Essentially, they extended the well-known classical theorem of corresponding states⁴ to include the effect of quantum mechanics and applied it to successfully predict the properties of He³, which had not yet been obtained experimentally at the time of their work. More recently, the QTCS has been used by Anderson and Palmer⁵ and Chao and Clark⁶ to estimate the properties of zero-temperature neutron matter and, in particular, to estimate its solidification pressure. This question, which is of primary importance in deciding what fraction (if any) of the interior of a given neutron star is crystalline neutron matter, has been studied by many authors⁷⁻¹⁶ with conflicting results. Its resolution is of fundamental importance for the understanding of neutron stars and is one of the major motivating factors for undertaking the present work. In the course of this study we believe that we have found a framework which is a most suitable one for studying the zero-temperature properties of all matter and will therefore be useful for the study of neutron matter, in particular.

In the present work we study extensively the zero-temperature properties of matter (interacting via a pair potential of the Lennard-Jones form) within the context of the QTCS. The main results of our calculations are given in Sec. V, in which we present calculations of the zero-temperature energy and pressure and of the nature of the liquid-solid phase transition. In many ways our results

are extensions of the results of Refs. 1-3. In particular, we find that the solidification pressure at zero temperature is strongly dependent upon whether or not the system obeys *Bose-Einstein* or *Fermi-Dirac* statistics. For example, if He³ particles were bosons, the solidification pressure would be greater by at least a factor of 2. From the curves presented in Fig. 10, it is clear that an extrapolation based on *one* curve, which, ignoring statistics, includes the solidification pressure for *both* He³ and He⁴, cannot yield even qualitatively significant results for larger η values.

The QTCS is discussed in Sec. II. We find that it is notationally convenient to use a parameter η [defined by Eq. (2.3c)] rather than the de Boer parameter Λ^* . The significance and value of this parameter are discussed in Sec. III. In particular, we show that it is illuminating to conceptually extend the space of thermodynamic variables to include η . In terms of this variable, one may derive analogs of all of the usual thermodynamic and statistical-mechanical relationships. In particular, phase transitions can take place at zero temperature as η is varied; this can be seen clearly in Figs. 8 and 9 in Sec. V. In this paper we study mainly first-order transitions, although in Appendix A we study briefly a model which exhibits a second-order transition as η is varied. We believe that further studies of phase transitions in this context would be most valuable.

Finally, all our conclusions are based upon calculations with systems for which the Lennard-Jones potential has been assumed. The question of how these conclusions would be changed for different potentials is an important one for future in-

vestigation. In particular, a study utilizing potentials such as describe the interaction between two nucleons would undoubtedly yield most interesting and important results.

II. QUANTUM THEOREM OF CORRESPONDING STATES

The QTCS, in essence, states that any thermodynamic function of a class of systems with a pair potential of the form

$$v(r) = \epsilon v^*(r/\sigma), \quad (2.1)$$

if written in terms of properly defined reduced variables, will be the *same* function of these variables for each system in this class. In (2.1) ϵ is the coupling constant (with dimensions of energy), σ is a range parameter (with dimensions of length), and $v^*(x)$ is the same dimensionless function of its argument for each member of this class of systems. In this paper, all of our numerical results will be for systems where $v(r)$ has the Lennard-Jones form; i.e.,

$$v^*(x) = 4(x^{-12} - x^{-6}). \quad (2.2)$$

To state the QTCS precisely, we introduce the following reduced variables:

$$T^* \equiv kT/\epsilon, \quad (2.3a)$$

where k is Boltzmann's constant and T is the temperature;

$$V^* \equiv V/N\sigma^3, \quad (2.3b)$$

where V is the volume and N is the number of particles;

$$\eta \equiv \hbar^2/m\epsilon\sigma^2, \quad (2.3c)$$

where \hbar is Planck's constant h divided by 2π and m is the mass. We have found this parameter notationally more convenient than the de Boer parameter Λ^* , where $\Lambda^* \equiv \hbar/(m\epsilon)^{1/2}\sigma$ and $\eta = (\Lambda^*/2\pi)^2$. Values of η , Λ^* , and the parameters for various systems and their pair potentials are given in Table I. The question of what these values should be for systems composed of nucleons is discussed in Refs. 5 and 6.

We may now give a precise statement of the QTCS. We will do it in terms of the Helmholtz free energy F (whose natural variables are T , V , and N), although any other thermodynamic potential would be just as satisfactory. It is that this free energy may be written

$$F = F(T, V, N) = \epsilon F^*(T^*, V^*, N, \eta), \quad (2.4)$$

where F^* (which we may call the reduced free energy) is a dimensionless function of its arguments with its functional form depending *only* on the form of $v^*(x)$ and on whether or not the particles obey

Bose-Einstein or *Fermi-Dirac* statistics. Thus, if the function F^* is known, all of the thermodynamic properties of the entire class of systems are known. Furthermore, if various experimental results are plotted in terms of these reduced variables, a simplified view of these systems often emerges.

For completeness, we shall now give a brief derivation of the QTCS. The Hamiltonian for the systems we will consider has the form

$$H = \frac{-\hbar^2}{2m} \sum_{i,\alpha} \left(\frac{\partial}{\partial r_{i\alpha}} \right)^2 + \sum_{i<j} v(r_{ij}), \quad (2.5)$$

where $\alpha = x, y, z$ and $r_{i\alpha}$ is the α th component of the position vector of the i th particle,

$$r_{ij}^2 = \sum_{\alpha} (r_{i\alpha} - r_{j\alpha})^2,$$

and we assume periodic boundary conditions for the cube $0 \leq r_{i\alpha} \leq L$, so that $V = L^3$. We may now make the transformation of variables $x_{i\alpha} \equiv r_{i\alpha}/\sigma$, so that the Hamiltonian may be written

$$H = \epsilon(\eta t + w). \quad (2.6)$$

Here the boundary conditions are now for the cube $0 \leq x_{i\alpha} \leq L/\sigma$ (or for the volume V/σ^3) and

$$t \equiv -\frac{1}{2} \sum_{i,\alpha} \left(\frac{\partial}{\partial x_{i\alpha}} \right)^2, \quad (2.7a)$$

$$w \equiv \sum_{i<j} v^*(x_{ij}), \quad (2.7b)$$

where

$$x_{ij}^2 = \sum_{\alpha} (x_{i\alpha} - x_{j\alpha})^2.$$

We may now consider the partition function Z in the canonical ensemble, although these considerations are valid for any statistical-mechanical ensemble. We have, using the first part of (2.4), (2.6), and the standard expressions for Z ,

TABLE I. Reduced quantum parameters Λ^* and η for various substances along with the mass (in amu, i.e., 1.66024×10^{-24} g), the coupling constant ϵ (in deg) and σ (in Å). We used $k = 1.38054 \times 10^{-16}$ erg/particle degree and $\hbar = 1.05450 \times 10^{-27}$ erg sec.

Substance	m	ϵ	σ	Λ^*	η
He ³	3.016	10.22	2.556	3.084	0.2409
He ⁴	4.003	10.22	2.556	2.677	0.1815
He ⁶	6.0	10.22	2.556	2.187	0.1211
H ₂	2.016	37.0	2.92	1.735	0.0763
Ne	20.18	35.6	2.74	0.4389	0.0049

$$\begin{aligned} Z &= Z(T, V, N) = \exp(-F/kT) \\ &= \text{Tr}[\exp(-H/kT)] \\ &= \text{Tr}\{\exp[-\epsilon(\eta t + w)/kT]\} \end{aligned} \quad (2.8a)$$

$$= Z^*(T^*, V^*, N, \eta), \quad (2.8b)$$

which follows by inspection and the boundary conditions for the $x_{i\alpha}$. The proof of the QTCS follows directly from the well-known formula

$$F = -kT \ln Z = -\epsilon T^* \ln Z^* \equiv \epsilon F^*. \quad (2.9)$$

Since the trace in (2.8) depends in an essential way on whether or not the particles obey *Bose-Einstein* or *Fermi-Dirac* statistics, the form of F^* (and, of course, Z^*) depends in an essential way on "the statistics." Thus, for a given $v^*(x)$, the QTCS may be viewed as treating *Bose-Einstein* and *Fermi-Dirac* systems as two different types of systems, each of which has a different dependence on the quantum parameter η .

III. THERMODYNAMICS AND STATISTICAL MECHANICS

In this section we wish to discuss and summarize many of the results which follow from the dependence of the free energy on the parameter η . From a conceptual point of view, this parameter (which depends only on the product $m\epsilon\sigma^2$) can be varied independently (e.g., one can visualize the mass varying). Thus, it is illuminating to extend the thermodynamic variable space to include an extra dimension for η (of course, if there were more than one component, there would be a different variable η for each component; the generalization to this case is straightforward). We may write

$$dF = -S dT - P dV + \mu dN + \varphi d\eta, \quad (3.1)$$

where S is the entropy, P is the pressure, μ is the chemical potential, and

$$\varphi \equiv \left(\frac{\partial F}{\partial \eta}\right)_{T, V, N}. \quad (3.2)$$

It turns out that φ has a simple physical interpretation. From (3.2) and (2.9) we have

$$\varphi = -kT \left(\frac{\partial Z}{\partial \eta}\right)_{T, V, N} / Z; \quad (3.3)$$

from which, with (3.8), we have

$$-\left[\left(\frac{V}{N}\right)_{\text{II}} - \left(\frac{V}{N}\right)_{\text{I}}\right] \left(\frac{\partial P}{\partial \eta}\right)_{\text{coexist}} = \left[\left(\frac{\varphi}{N}\right)_{\text{II}} - \left(\frac{\varphi}{N}\right)_{\text{I}}\right] + \left[\left(\frac{S}{N}\right)_{\text{I}} - \left(\frac{S}{N}\right)_{\text{II}}\right] \left(\frac{\partial T}{\partial \eta}\right)_{\text{coexist}}. \quad (3.10)$$

Clearly, (3.10) is the generalization of the Clausius-Clapeyron equation. It is straightforward to generalize all of the usual thermodynamic relationships to this case.

however, from (2.8a) we have

$$\left(\frac{\partial Z}{\partial \eta}\right)_{T, V, N} = \text{Tr} \left(\frac{\partial \exp[-\epsilon(\eta t + w)/kT]}{\partial \eta} \right), \quad (3.4)$$

since the trace can be taken over an arbitrary set of states; this result is just the finite-temperature version of the Feynman-Hellmann theorem.¹⁷ If we now complete the differentiation in (3.4) and use (3.3), we find

$$\varphi = \epsilon \langle t \rangle = \langle K \rangle / \eta, \quad (3.5)$$

where K is the kinetic-energy part of the Hamiltonian and the $\langle \rangle$ indicate the thermodynamic average.

We may also consider the case where φ is the independent variable instead of η . Then we may consider the thermodynamic potential

$$\mathcal{F} = F - \eta\varphi = \mathcal{F}(T, V, N, \varphi) \quad (3.6a)$$

$$= \langle H \rangle - TS - \eta\varphi = \epsilon \langle w \rangle - TS, \quad (3.6b)$$

so that, at zero temperature, \mathcal{F} is just the average potential energy $\bar{W} = \bar{W}(V^*, N, \varphi)$. It is straightforward to construct the ensemble for which \mathcal{F} is the natural potential; one finds

$$\mathfrak{g} = \exp(-\mathcal{F}/kT) = \int_0^\infty d\eta \text{Tr} \left[\exp\left(\frac{-(H - \eta\varphi)}{kT}\right) \right]. \quad (3.7)$$

This ensemble has the physical significance of considering systems with all possible values of η (e.g., with all possible masses) and selecting the one of interest by choosing φ . Perhaps there are problems for which this ensemble is especially well suited.

Since we wish to use this formalism to investigate phase transitions, it is useful to write down some of the relevant thermodynamic relationships. First, there is the analog of the Gibbs-Duhem relationship,

$$N d\mu = -S dT + V dP + \varphi d\eta. \quad (3.8)$$

When two phases (say I and II) are coexisting, we have

$$\mu_{\text{I}} = \mu_{\text{II}}, \quad (3.9)$$

Since all of the results which will be presented in this paper are for the case of zero temperature only, it is worthwhile to summarize the relevant thermodynamic quantities and relationships for

this special case. We may define E^* (the reduced energy per particle) and P^* (the reduced pressure) by

$$E^* \equiv E/N\epsilon, \quad (3.11a)$$

$$P^* \equiv P\sigma^3/\epsilon. \quad (3.11b)$$

It follows from (2.4) that, at zero temperature,

$$E^* = E^*(V^*, \eta), \quad (3.12a)$$

$$P^* = -\left(\frac{\partial E^*}{\partial V^*}\right)_\eta = P^*(V^*, \eta). \quad (3.12b)$$

We may also consider K^* and W^* (respectively, the reduced average kinetic and potential energies per particle).

There are several quantities which are particularly easy to discuss at zero temperature, because they depend only on η . They are (a) V_0^* (the reduced volume at zero pressure), (b) P_s^* (the reduced solidification pressure), (c) V_L^* (the reduced volume of the liquid at P_s^*), and (d) V_s^* (the reduced volume of the crystal at P_s^*).

Equation (3.10) may also be simplified at zero temperature, whence it may be written

$$\left(\frac{\partial P^*}{\partial \eta}\right)_{\text{coexist}} = -\frac{(\varphi_I^* - \varphi_{II}^*)}{(V_I^* - V_{II}^*)}. \quad (3.13)$$

Thus, the slope of the coexistence curve in the $P^* - \eta$ plane is determined by the difference in kinetic energy divided by the volume difference, just as the slope of the coexistence curve in the $P - T$ plane is determined by the entropy difference, again divided by the volume difference.

We also wish to point out that it is possible to give another view of the QTCS for the Lennard-Jones potential. Let us consider the potential

$$v(r) = 4\epsilon[(\sigma/r)^{12} - \nu(\sigma/r)^6], \quad (3.14)$$

where ν can be varied to adjust the attractive part of the potential; in particular, in the limit $\nu \rightarrow 0$, the potential becomes purely repulsive. Now (3.14) can also be written as

$$v(r) = 4\bar{\epsilon}[(\bar{\sigma}/r)^{12} - (\bar{\sigma}/r)^6], \quad (3.15)$$

where

$$\bar{\epsilon} \equiv \nu^2\epsilon, \quad \bar{\sigma} \equiv \sigma/\nu^{1/6}. \quad (3.16)$$

Thus, the QTCS holds for a class of systems such that

$$\bar{\eta} = \hbar^2/m\bar{\epsilon}\bar{\sigma}^2 = \eta/\nu^{5/3}, \quad (3.17)$$

so that for a Lennard-Jones potential a change in η can also be viewed as a change in the relative strength of the attractive part of the interaction with m , ϵ , and σ all held fixed. In this case, the various reduced quantities become

$$\bar{E}^* = E^*/\nu^2, \quad (3.18a)$$

$$\bar{V}^* = V^*\nu^{1/2}, \quad (3.18b)$$

$$\bar{P}^* = \nu^{3/2}P^*. \quad (3.18c)$$

Therefore, the asymptotic values of the various reduced quantities in the limit $\eta \rightarrow \infty$ will yield the behavior of these quantities for a system with a pure r^{-12} repulsion.

IV. METHOD OF CALCULATION

Our calculation is patterned after (and uses many of the results of) those of McMillan,¹⁸ Schiff and Verlet¹⁹ (hereafter referred to as SV), and Hansen and co-workers^{20, 21} (hereafter Ref. 20 is referred to as HL). One virtue of this approach is that similar approximations are used in calculating the ground-state energies of *both* the liquid and crystalline phases. In particular, the results²⁰ for the solidification pressure of He³ and He⁴ are in reasonably good agreement with experiment.

The problem is formulated as a variational calculation of the ground-state energy using trial wave functions of the form

$$\psi = F\phi. \quad (4.1)$$

In all cases

$$F = F(\vec{r}_1, \dots, \vec{r}_N; b) = \prod_{i < j} \exp\left[-\frac{1}{2}\left(\frac{b}{r_{ij}}\right)^5\right], \quad (4.2)$$

where b is a variational parameter. This factor F is introduced to take into account the effect of short-range correlations due to the strong short-range repulsion between two atoms. The particular properties of a given phase and the effects of the quantum statistics are introduced via the choice of the function ϕ . The usual choices are as follows:

$$\phi = 1 \quad (4.3a)$$

for a Bose liquid;

$$\phi = \mathcal{A}\left[\prod_j \exp(i\vec{r}_j \cdot \vec{k}_j)\xi_j\right] \quad (4.3b)$$

for a Fermi liquid, where the wave vectors \vec{k}_j and spin functions ξ_j are chosen to fill the Fermi sea and \mathcal{A} is the antisymmetrizer; and

$$\phi_c = \prod_j \exp[-\frac{1}{2}A(\vec{r}_j - \vec{R}_j)^2] \quad (4.3c)$$

for both Bose and Fermi crystals, where \vec{R}_j is the position of the equilibrium site of the j th particle and A is a variational parameter. The effects of symmetrizing or antisymmetrizing the wave function have been neglected in the choice of ϕ for a crystal because the exchange energies are negligibly small in the crystals being considered.

Given this formulation, it is straightforward to construct the expressions for the ground-state energies of the various systems.^{19, 20} An important point, which is fully discussed in SV and by Wu and Feenberg,²² is the use of cluster-expansion techniques to calculate the effect of antisymmetrization for liquid He³. Furthermore, as pointed out first by McMillan,¹⁸ a complete set of calculations at one density ρ (which we shall call the *reference density* ρ_0) enables calculations to be made at *all* densities by means of a simple scaling procedure. Fortunately, extensive tables of the results of these calculations were published^{19, 20} and we have utilized these results for the present investigation. It was necessary to augment their results with our own calculations. The combined results are presented in Tables II and III. In addition, we have fitted these results with polynomials in order to minimize the effect of scatter due to statistical error in the Monte Carlo calculations and also to provide a means of interpolating between entries in the table. This fitting procedure and the numerical results are given in Appendix B.

We shall now write down the energy expressions for the liquid and solid in a form such that the scaling property is given explicitly. Following SV we introduce the scaling parameter S defined by

$$\rho = S^3 \rho_0, \quad (4.4)$$

which relates the tabulated results at the reference density ρ_0 to results at any other density ρ . The basic scaling equation for Lennard-Jones systems is, in terms of the reduced parameters of the QTCS,

$$E^*(\rho; A, b) = \eta S^2 \langle t/N \rangle_0 + 4[S^{12} \langle (\sigma/r)^{12} \rangle_0 - S^6 \langle (\sigma/r)^6 \rangle_0], \quad (4.5)$$

where $\eta \langle t/N \rangle_0$ is the reduced kinetic energy and $4 \langle (\sigma/r)^n \rangle_0$ is the reduced energy associated with the r^{-n} term in the Lennard-Jones potential. The subscript on the expectation values indicates that they are evaluated at the reference density ρ_0 with variational parameters (A_0, b_0) . The reduced energy at the scaled density ρ is then given for the scaled variational parameters (A, b) , where

$$A = S^2 A_0, \quad (4.6a)$$

$$b = b_0 / S. \quad (4.6b)$$

In reduced form, $A^* = A\sigma^2$ and $b^* = b/\sigma$. Of course, there is no A parameter for the liquid variational wave function.

The explicit expression for the expectation values depends upon the phase and statistics of the system. The energy for the liquid phase is conveniently expressed in terms of the Bose radial distribution function:

$$g_B(r; \rho, b) \equiv \rho^{-2N} (N-1) \frac{\int d\vec{r}_3 \dots \int d\vec{r}_N F^2(\vec{r}_1, \dots, \vec{r}_N; b)}{\int d\vec{r}_1 \dots \int d\vec{r}_N F^2(\vec{r}_1, \dots, \vec{r}_N; b)} \quad (4.7)$$

Then the expectation values of inverse powers of r for the Bose liquid are given by

$$\langle (\sigma/r)^n \rangle_{LB,0} = \frac{1}{2} \rho_0 \int d\vec{r} g_B(r; \rho_0, b_0) (\sigma/r)^n. \quad (4.8)$$

For the Bose liquid the expectation value associated with the reduced kinetic energy is simply

$$\langle t/N \rangle_{LB,0} = 5b_0^* \langle (\sigma/r)^7 \rangle_{LB,0}. \quad (4.9)$$

The scaling equation for the reduced energy of the Bose liquid is then

$$E_{LB}^*(\rho; b) = 5\eta S^2 b_0^* \langle (\sigma/r)^7 \rangle_{LB,0} + 4[S^{12} \langle (\sigma/r)^{12} \rangle_{LB,0} - S^6 \langle (\sigma/r)^6 \rangle_{LB,0}]. \quad (4.10)$$

The three expectation values for the Bose liquid are tabulated in Table I of SV at a reference density $\rho_0 = 0.01967$ atoms/ \AA^3 (0.3283 atoms/ σ^3) and are reproduced with some additions in our Table II.

The energy expression for a Fermi liquid involves additional terms due to the Fermi energy and various exchange energies. The expectation values of $(\sigma/r)^n$ are given by

$$\langle (\sigma/r)^n \rangle_{LF,0} = \langle (\sigma/r)^n \rangle_{LB,0} - \langle (\sigma/r)^n \rangle_{LX,0}, \quad (4.11)$$

where the exchange integral is

$$\langle (\sigma/r)^n \rangle_{LX,0} = \frac{1}{4} \rho_0 \int d\vec{r} g_B(r; \rho_0, b_0) h^2(k_{F0} r) (\sigma/r)^n, \quad (4.12)$$

with $h(x) = 3(\sin x - x \cos x)/x^3$. The expectation value associated with the reduced kinetic energy of the Fermi liquid is

$$\langle t/N \rangle_{LF,0} = \frac{3}{10} k_{F0}^* \langle (\sigma/r)^7 \rangle_{LF,0}, \quad (4.13)$$

where k_{F0} is the Fermi wave number at the reference density, $k_{F0}^* \equiv k_{F0} \sigma$, and the exchange single-particle kinetic energy is determined by

$$\epsilon_{x,0}^* = -20 \int_0^1 dy y^4 (1 - \frac{3}{2}y + \frac{1}{2}y^3) u_B(2k_{F0} y; \rho_0, b_0), \quad (4.14)$$

with

$$u_B(k; \rho, b) \equiv \rho \int d\vec{r} \exp(i\vec{k} \cdot \vec{r}) [g_B(r; \rho, b) - 1]. \quad (4.15)$$

Thus the scaling equation for the Fermi-liquid reduced energy is

$$\begin{aligned}
E_{LF}^*(\rho, b) = & E_{LB}^*(\rho, b) + \frac{3}{10}\eta S^2 k_{F0}^* (1 - \epsilon_{*0}^*) \\
& - 5\eta S^2 b_0^{*5} \langle (\sigma/r)^7 \rangle_{LX,0} \\
& - 4[S^{12} \langle (\sigma/r)^{12} \rangle_{LX,0} - S^6 \langle (\sigma/r)^6 \rangle_{LX,0}].
\end{aligned} \tag{4.16}$$

The exchange terms in (4.16) were not tabulated in SV. We have therefore included them in our Table II only for those b_0 values calculated by the present authors. We have included in (4.16) only terms up through the two-particle term in the cluster expansion with respect to statistics, since it was shown in SV that higher terms have a small effect upon the ground-state energy.

Finally, we present the scaling equation for the ground-state energy of the crystal. This expres-

where

$$G_j(r_{1j}; \rho, A, b) = \frac{\int d\vec{r}_{1j} \int d\vec{R}_{1j} \int d\vec{r}_2 \dots \int d\vec{r}_{j-1} \int d\vec{r}_{j+1} \dots \int d\vec{r}_N F^2 \phi_c^2}{4\pi \int d\vec{r}_1 \dots \int d\vec{r}_N F^2 \phi_c^2}, \tag{4.19}$$

with

$$\vec{R}_{1j} \equiv (\vec{r}_1 + \vec{r}_j)/2, \quad \vec{r}_{1j} = \vec{r}_1 - \vec{r}_j. \tag{4.20}$$

The expectation values of $(\sigma/r)^n$ in the crystal are given in Table I of HL. We have supplemented these numbers with additional entries necessary in this study and present all cases in our Table III at a reference density of $\rho_0 = 0.02803 \text{ atom/\AA}^3$ ($0.4680 \text{ atom}/\sigma^3$).

With these scaling equations for the reduced energies and the available tables, it is a straightforward matter to calculate E^* as a function of V^* and η . These results and an analysis are given in Sec. V.

V. RESULTS AND DISCUSSION

In this section we present the results of our calculations. They are all based upon calculations of E^* as a function of V^* and η . In Figs. 1-4 we present, in each case, $E^*(V^*)$ for the Fermi liquid, the Bose liquid, and for the crystal for four different values of η . In each case, the energy of the Fermi liquid is higher than that of the Bose liquid, mainly due to the Fermi energy. As we mentioned in Sec. IV, this effect is not important for the crystals because the exchange energy is so small. From these curves it is intuitively clear that relative to the crystalline phase the Fermi liquid is less stable than the Bose liquid; i.e., the Fermi liquid will crystallize at a lower pressure than the Bose liquid for the same value of η . In fact, our results suggest that if He⁴ had been a fermion, it might very well have been a crystal at zero temperature!

In Fig. 1 we present the curves for η sufficiently

small so that the crystalline phase is stable for both fermions and bosons at all pressures. In Fig. 2 we present the curves for $\eta = \eta_B = 0.171$, the value of η for which the Bose liquid and crystal coexist at zero temperature and pressure; for values of $\eta > \eta_B$, the ground state of the Bose system at zero temperature and pressure is a liquid. In Fig. 3 we present the curves for $\eta = \eta_F = 0.197$, the value of η for which the Fermi liquid and crystal coexist at zero temperature and pressure. On this graph we also show the Maxwell construction which yields P_s^* for the Bose system. In Fig. 4 we present the curves for $\eta = 0.260$, which is somewhat greater than the value of η for He³. Clearly, P_s^* for a Fermi system is much lower than that for a Bose system with the same value of η . In Fig. 5 we present E_0^* as a function of η . This graph (which should be compared with Fig. 2 of Ref. 1) shows clearly the difference between the Fermi and Bose systems and also the discontinuity in ϕ^* which shows that one may view the situation as a first-order phase transition in the $E_0^* - \eta$ plane.

$$\begin{aligned}
E_c^*(\rho; A, b) = & \eta S^2 [\frac{3}{4}A_0^* + 5b_0^{*5} \langle (\sigma/r)^7 \rangle_{c,0}] \\
& + 4[S^{12} \langle (\sigma/r)^{12} \rangle_{c,0} - S^6 \langle (\sigma/r)^6 \rangle_{c,0}],
\end{aligned} \tag{4.17}$$

where the expectation values are evaluated using (4.8) with the liquid distribution function $g_B(r; \rho, b)$ replaced by a spherically averaged radial distribution function for the crystal, namely,

$$g_c(r; \rho, A, b) \equiv \frac{1}{\rho} \sum_{j \geq 2} G_j(r; \rho, A, b), \tag{4.18}$$

small so that the crystalline phase is stable for both fermions and bosons at all pressures. In Fig. 2 we present the curves for $\eta = \eta_B = 0.171$, the value of η for which the Bose liquid and crystal coexist at zero temperature and pressure; for values of $\eta > \eta_B$, the ground state of the Bose system at zero temperature and pressure is a liquid. In Fig. 3 we present the curves for $\eta = \eta_F = 0.197$, the value of η for which the Fermi liquid and crystal coexist at zero temperature and pressure. On this graph we also show the Maxwell construction which yields P_s^* for the Bose system. In Fig. 4 we present the curves for $\eta = 0.260$, which is somewhat greater than the value of η for He³. Clearly, P_s^* for a Fermi system is much lower than that for a Bose system with the same value of η . In Fig. 5 we present E_0^* as a function of η . This graph (which should be compared with Fig. 2 of Ref. 1) shows clearly the difference between the Fermi and Bose systems and also the discontinuity in ϕ^* which shows that one may view the situation as a first-order phase transition in the $E_0^* - \eta$ plane.

In Figs. 6 and 7 we plot V^* as a function of η for the Fermi and Bose systems, respectively. We may compare these graphs with Fig. 1 of Ref. 1. Clearly, as η increases V_0^* (the reduced volume at zero pressure) also increases, indicating that one may view the effect of the zero-point motion as causing the particles to behave as if they were "larger" than the potential would indicate. De Boer² describes this as a "blowing up" of the particles due to a repulsive internal pressure generated by the zero-point kinetic energy. On these two graphs we also plot V_s^* and V_c^* , the reduced volumes of the coexisting fluid and crystal at the

solidification pressure P_s^* . There are two significant features of these curves: (a) Unlike V_0^* , V_L^* and particularly V_s^* appear to approach a constant value as η increases beyond its critical value; and (b) although V_L^* and V_s^* are approximately independent of η , they are still considerably larger than the "core" of the potential would suggest. While $V_s^* \cong 2$, the reduced volume for close packing at a nearest-neighbor distance of the core diameter, σ , is $V^* = 0.707$. This is the reduced volume one might expect for the classical ($\eta = 0$) system at

very high pressure. The classical reduced volume at zero pressure is $V_0^*(\eta = 0) = 0.916$, which is only slightly larger than the close-packing volume and still much smaller than the solidification volume V_s^* of the quantum solid. Thus while at zero pressure the apparent "size" of the quantum particles "blows up" with increasing η due to the zero-point kinetic energy, there seems to be a definite size below which the particles may not be compressed and remain in the liquid phase. That this minimum "size" is considerably larger than the core size is

TABLE II. Values of $r_n^* \equiv \langle (\sigma/r)^n \rangle_{LB}$, $r_{nx}^* \equiv \langle (\sigma/r)^n \rangle_{LX}$, and ϵ_x^* for the fluid for different values of the variational parameter $b^* = \bar{b}/\sigma$; all quantities are dimensionless. The reference density $\rho_0 = 0.01967$ atoms/ \AA^3 . Those quantities for which there are "exchange" averages were generated for the present work; the rest are reproduced from Table I of SV.

b^*	r_6^*	r_{6x}^*	r_7^*	r_{7x}^*	r_{12}^*	r_{12x}^*	ϵ_x^*
0.9880	1.0028		0.8753		0.9415		
0.9940	0.9914		0.8648		0.8928		
1.0140	0.9601	0.1226	0.8151	0.1226	0.8070	0.1760	0.010 74
1.0150	0.9550		0.8076		0.7873		
1.0360	0.9210		0.7660		0.6876		
1.0490	0.8898	0.1050	0.7322	0.1019	0.6059	0.1235	0.011 22
1.0560	0.8910		0.7338		0.6062		
1.0770	0.8626		0.7006		0.5380		
1.0840	0.8477	0.0949	0.6842	0.0906	0.5072	0.0988	0.011 58
1.0980	0.8367		0.6698		0.4763		
1.1190	0.8124		0.6418		0.4225		
1.1190	0.8070	0.0854	0.6383	0.0798	0.4195	0.0775	0.011 91
1.1390	0.7897		0.6177		0.3766		
1.1600	0.7690		0.5934		0.3385		
1.1600	0.7612	0.0750	0.5878	0.0686	0.3375	0.0587	0.012 37
1.1810	0.7468		0.5701		0.3051		
1.2010	0.7274		0.5505		0.2769		
1.2010	0.7205	0.0659	0.5434	0.0588	0.2705	0.0438	0.012 80
1.2220	0.7096		0.5312		0.2526		
1.2430	0.6934		0.5128		0.2296		
1.2640	0.6780		0.4956		0.2100		
1.2640	0.6746	0.0563	0.4950	0.0489	0.2098	0.0312	0.013 37
1.2840	0.6642		0.4820		0.1935		
1.2840	0.6602	0.0534	0.4801	0.0459	0.1934	0.0280	0.013 62
1.2970	0.6537		0.4717		0.1831		
1.3050	0.6512		0.4677		0.1771		
1.3050	0.6446	0.0502	0.4639	0.0427	0.1749	0.0243	0.013 79
1.3260	0.6383		0.4544		0.1640		
1.3360	0.6280	0.0469	0.4469	0.0394	0.1575	0.0210	0.014 08
1.3460	0.6269		0.4400		0.1509		
1.3670	0.6164		0.4326		0.1378		
1.3670	0.6111	0.0435	0.4295	0.0361	0.1398	0.0177	0.014 36
1.3880	0.6067		0.4221		0.1312		
1.4090	0.5970		0.4123		0.1214		
1.4090	0.5899	0.0396	0.4085	0.0323	0.1216	0.0145	0.014 71
1.4290	0.5881		0.4039		0.1115		
1.4500	0.5791		0.3950		0.1050		
1.4500	0.5727	0.0363	0.3913	0.0291	0.1067	0.0119	0.015 02
1.4850	0.5571	0.0336	0.3764	0.0267	0.0958	0.0010	0.015 39
1.5200	0.5461	0.0315	0.3655	0.0247	0.0876	0.0089	0.015 60
1.5600	0.5314	0.0291	0.3516	0.0225	0.0781	0.0074	0.015 97
1.6000	0.5203	0.0273	0.3412	0.0209	0.0718	0.0065	0.016 21

a manifestation of quantum effects. We should note that the remarkable insensitivity to η of V_s^* (and to a lesser extent V_L^*) may be a specific property of the relatively hard core of the Lennard-Jones potential. This property needs to be investigated for softer-core potentials such as the Yukawa core of the nuclear potential. The fact that V_s^* is larger for the fermion system than the Bose system indicates that the quantum statistics also affects this minimum "size" V_s^* .

In Fig. 8 and 9 we plot P^* versus V^* for various values of η for both Fermi and Bose systems. The curves look very much like those for P - V isotherms for gases. There are two differences. One is that there is a finite volume at zero pressure. The other is that this seems to be no critical point, which is, of course, expected for a liquid-solid transition. Finally, in Fig. 10 we plot P_s^* versus η for both Fermi and Bose systems. Again P_s^*

TABLE III. Values of $r_{nc}^* \equiv \langle (\sigma/r)^n \rangle_c$ for the crystal for different values of the variational parameters $b^* = b/\sigma$ and $A^* = A\sigma^2$; all quantities are dimensionless. The reference density $\rho_0 = 0.02803$ atoms/ \AA^3 . The first four entries were calculated for the present work; the remaining were taken from Table I of HL with the fifth through thirteenth entries scaled from $\rho = 0.02515$ atoms/ \AA^3 to this reference density.

b^*	A^*	r_{6c}^*	r_{7c}^*	r_{12c}^*
1.0032	4.2992	1.3865	1.1687	1.0542
1.0224	3.7618	1.3822	1.1606	1.0004
1.0224	5.3740	1.2861	1.0500	0.7873
1.0417	4.8366	1.2942	1.0579	0.7896
1.0610	4.2992	1.2714	1.0251	0.7386
1.0610	6.4488	1.1891	0.9310	0.5761
1.0803	3.2244	1.2976	1.0534	0.7756
1.0803	4.2992	1.2462	0.9959	0.6732
1.0803	5.3740	1.2017	0.9454	0.5892
1.0803	6.9863	1.1573	0.8944	0.5095
1.0996	4.2992	1.2152	0.9620	0.6094
1.0996	5.3740	1.1773	0.9172	0.5339
1.0996	6.9863	1.1317	0.8720	0.4665
1.1400	4.0000	1.1937	0.9310	0.5397
1.1400	5.0000	1.1598	0.8923	0.4825
1.1400	6.0000	1.1317	0.8609	0.4369
1.1600	3.0000	1.2072	0.9454	0.5534
1.1600	4.0000	1.1649	0.8981	0.4845
1.1600	5.0000	1.1372	0.8673	0.4409
1.1600	6.0000	1.1132	0.8400	0.4050
1.1600	7.0000	1.0923	0.8173	0.3741
1.1600	9.0000	1.0548	0.7787	0.3407
1.1800	4.0000	1.1454	0.8764	0.4496
1.2000	3.5000	1.1420	0.8732	0.4400
1.2000	4.0000	1.1280	0.8569	0.4190
1.2000	4.5000	1.1100	0.8376	0.3940
1.2000	5.0000	1.1000	0.8261	0.3790
1.2000	6.0000	1.0820	0.8069	0.3560
1.2400	4.0000	1.0894	0.8152	0.3595
1.3000	6.0000	1.0085	0.7281	0.2535

is much smaller for the Fermi system. Furthermore, the graph is remarkably linear, although we have been able to attach no significance to this result.

Since we have utilized well-known methods and published results,¹⁸⁻²¹ our results for the properties of both isotopes of helium are the same as those results. A comparison of these results with experiment is given in Ref. 20; it is found that the agreement between theory and experiment is quite reasonable. The most notable discrepancy is that the calculated volume change upon solidification He⁴ ($\Delta V_{\text{calc}}^* = V_L^* - V_s^* = 0.82$) is larger than the experimental volume change ($\Delta V_{\text{expt}}^* = 0.22$), so that the calculated He⁴ solidification pressure ($P_s^* = 0.083$) is lower than experiment ($P_s^* = 0.30$). Nevertheless, the generally good agreement between theory and experiment for these two isotopes indicates that this calculation will give a qualitatively correct description of zero-temperature properties of Lennard-Jones systems with even larger quantum parameters.

However, it is clear that one can not employ the

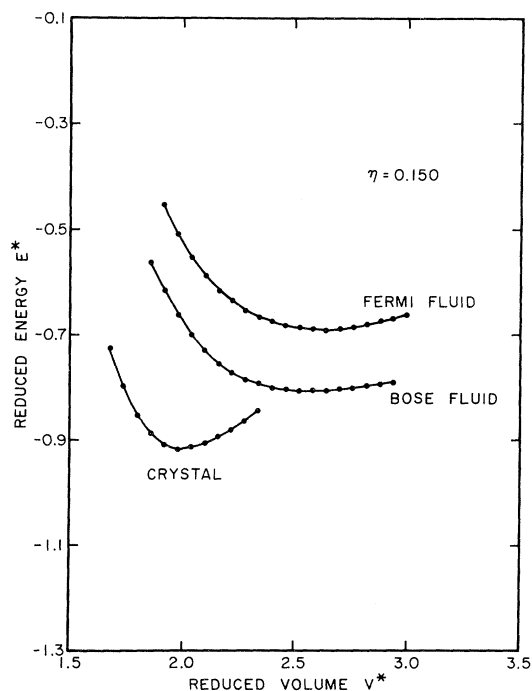


FIG. 1. Reduced ground-state energy E^* as a function of the reduced volume V^* for the fluid and crystalline phases of a Lennard-Jones system with a quantum parameter of $\eta = 0.150$. The results for both Fermi-Dirac and Bose-Einstein statistics are shown. The crystalline curve is insensitive to statistics. This value of η is sufficiently classical, i.e., small, that the stable phase of such a system at zero pressure and temperature would be crystalline.

methods used in this paper to study systems with arbitrarily large values of the quantum parameter η . As this parameter increases, the value of the parameter A which minimizes the solid energy at a particular volume decreases. This means that the exchange energy in the solid increases as the quantum parameter increases. The present method ignores exchange in the solid and is therefore limited to values for which the exchange energy is negligible. In addition, the usefulness of the present parametrization of the variational wave function has been demonstrated only for $\eta = 0.18$ and 0.24 . It is not likely that this parametrization will be adequate for very large values of η . Therefore, the present study has been limited to volumes V^* and quantum parameters for which the values of the variational parameters A^* and b^* that minimize the energy, when scaled to the reference density, lie within the range of parameters tabulated by HL and SV. For this range of parameters the exchange energy is negligible and the variational approach used in the present work has been shown to yield good results.

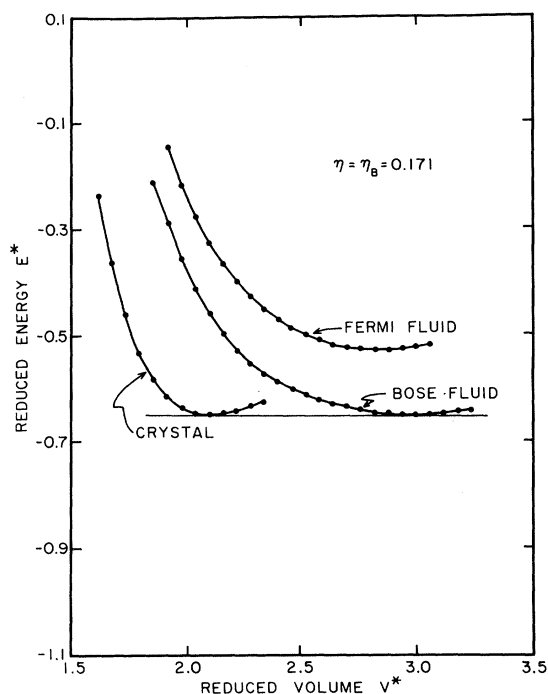


FIG. 2. Same graph as in Fig. 1 but for a value of $\eta = \eta_B = 0.171$, which is exactly the critical value for Bose-Einstein statistics. For this η the liquid and crystalline phases of a Bose-Einstein will coexist at zero temperature and pressure and only the crystalline phase of Fermi-Dirac system would be stable.

In concluding this section, we can say that the properties of matter at zero temperature show many similarities to the properties of matter at finite temperature. These results raise many questions. In the first place, is there also a liquid-gas transition at zero temperature? We expect that there should be; after all, if η is sufficiently large, the kinetic energy will dominate the system and this is the main characteristic of a gas. Would there be a critical point with the kind of singular behavior observed in real gas-liquid transitions? We believe that this is an important point for further investigation. Finally, all of our results are based on Lennard-Jones-type potentials where the distance of the minimum is about 10% larger than the core diameter. What would these curves look like for potentials of different form or with potentials with exchange interactions such as exist in nucleon matter? Again we believe that these are important points for further investigation.

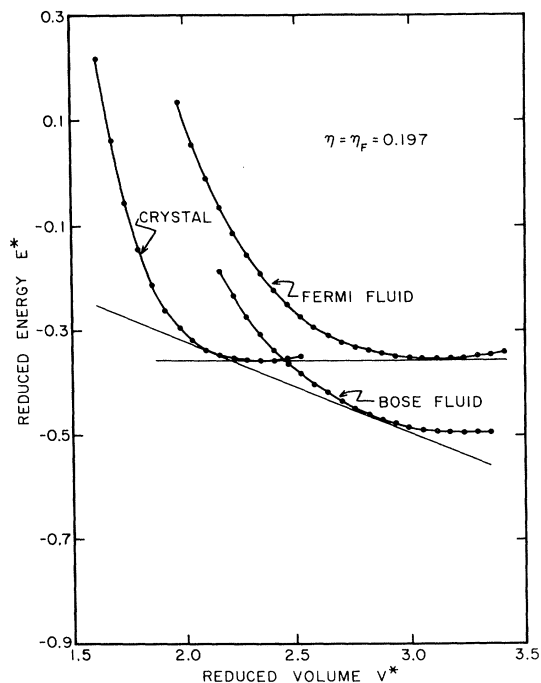


FIG. 3. Same graph as in Figs. 1 and 2, but for a value of $\eta = \eta_F = 0.197 > \eta_B$, which is exactly the critical value for Fermi-Dirac statistics. For this η the liquid and crystalline phases of a Fermi-Dirac system will coexist at zero temperature and pressure, and the equilibrium phase of a Bose-Einstein system would be fluid. The pressure required to solidify the Bose system is determined by the slope of the common tangent to the crystalline and Bose fluid curves, which is also shown.

ACKNOWLEDGMENTS

The authors wish to acknowledge helpful conversations with Dr. R. L. Coldwell. We also wish to acknowledge help and financial assistance from the computer systems of both the University of Minnesota and the University of Florida.

APPENDIX A

In this Appendix we wish to consider a simple model which exhibits a second-order phase transition as η is varied. It is one version of the well-known Stoner-Slater model where the interaction energy may be written

$$E_{\text{int}} = v_0 N_+ N_- / V, \quad (\text{A1})$$

where N_+ (N_-) is the number of up (down) spins, so that

$$N = N_+ + N_-. \quad (\text{A2})$$

and

$$v_0 = \int d\vec{r} v(r) = \epsilon \sigma^3 \int d\vec{x} v^*(x) \equiv \epsilon \sigma^3 v_0^*. \quad (\text{A3})$$

Since the model allows for an up- and a down-spin Fermi sea, one may write the reduced energy as ($k_F^* = k_F \sigma$, k_F is the Fermi momentum)

$$E^* = \left(\frac{3}{20}\right) \eta (k_F^*)^2 [(1 + \delta)^{5/3} + (1 - \delta)^{5/3}] \quad (\text{A4})$$

$$+ (1 - \delta^2) v_0^* / 4 V^* \\ \cong E_n^* + \frac{1}{2} A \delta^2 + \frac{1}{4} B \delta^4, \quad (\text{A5})$$

where

$$N_{\pm} = \frac{1}{2} N (1 \pm \delta), \quad \delta \geq 0, \quad (\text{A6a})$$

$$E_n^* = \frac{3}{10} \eta (k_F^*)^2 + v_0^* / 4 V^*, \quad (\text{A6b})$$

$$A = \frac{1}{3} \eta (k_F^*)^2 - v_0^* / 2 V^*, \quad (\text{A6c})$$

$$B = \eta (k_F^*)^2 / 40.5. \quad (\text{A6d})$$

Clearly (A5) is in the usual Landau-theory form and (A6c) shows that A can vanish for a critical value of η (say, η_c) as it does for a critical value

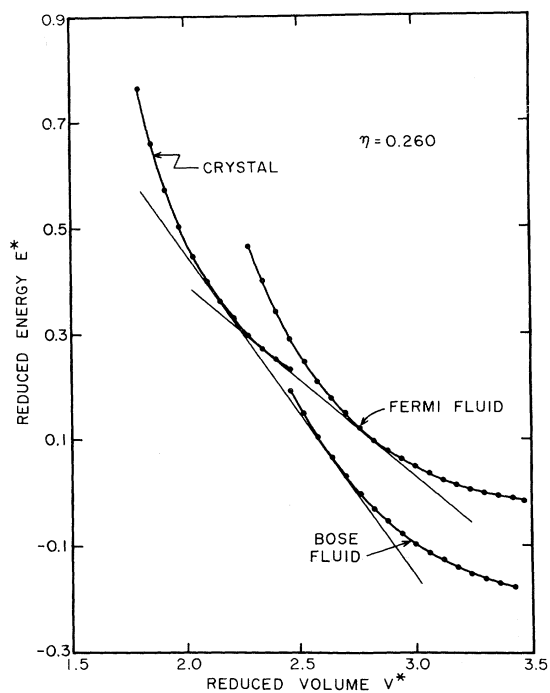


FIG. 4. Same graph as in Figs. 1-3 with a quantum parameter greater than the critical value for either Fermi-Dirac or Bose-Einstein statistics; here $\eta = 0.260$, which is slightly greater than quantum parameter for He^3 [$\eta_{(\text{He}^3)} = 0.2409$]. For this η the equilibrium phase for either Fermi or Bose statistics is fluid. The common tangent to the crystalline and fluid curve is shown for both statistics. Note that, as indicated in the text, the solidification pressure for Fermi statistics is lower than that for Bose statistics.

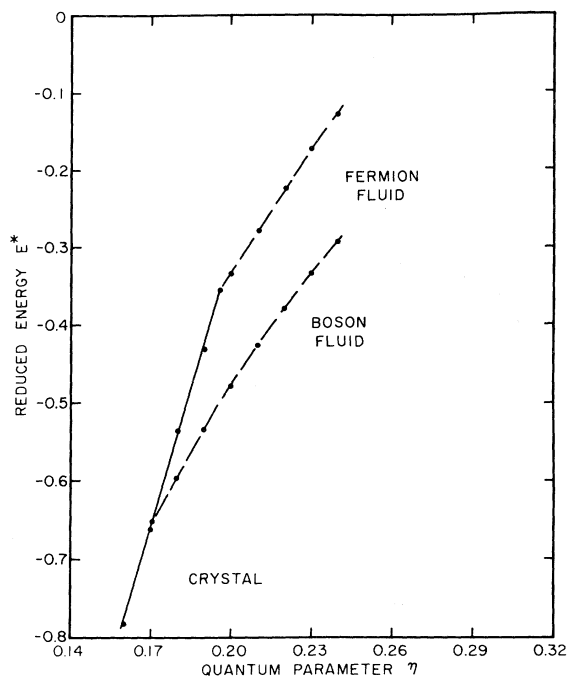


FIG. 5. Reduced ground-state energy at zero pressure E_0^* as a function of the quantum parameter η for systems with a Lennard-Jones potential. The results for both Fermi-Dirac and Bose-Einstein statistics are shown. The two branches correspond to Fermi and Bose fluids. These branches meet the crystalline curve (the crystal is insensitive to statistics) with a definite change in slope indicating a first-order phase transition at a critical value of η which is dependent upon statistics.

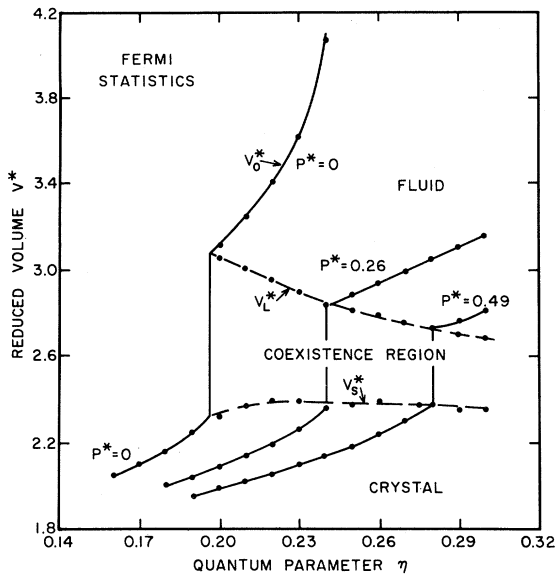


FIG. 6. Reduced volume at zero temperature as a function of the quantum parameter η for zero pressure V_0^* and pressure at which the fluid V_L^* and crystal V_S^* coexist. These curves are for systems with Fermi-Dirac statistics and a Lennard-Jones two-body potential. Note that if V_0^* were extended to the classical limit, $\eta=0$, then assuming an fcc lattice, $V_0^*(\eta=0)=0.916$.

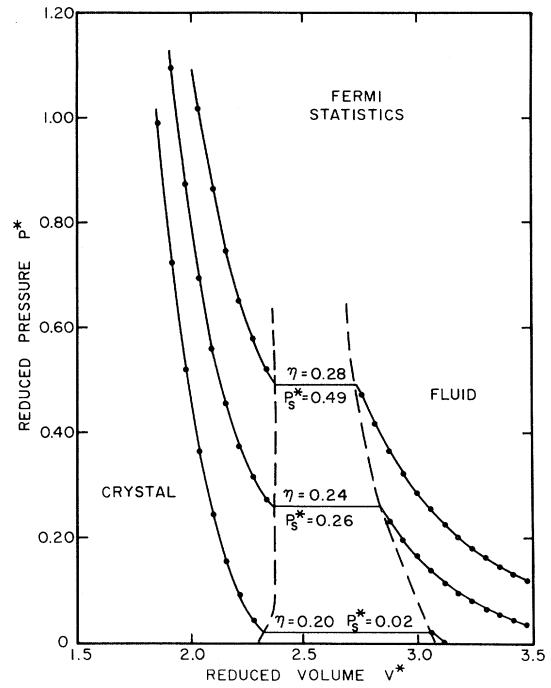


FIG. 8. P^*-V^* diagram with lines of constant η for Lennard-Jones systems at zero temperature with Fermi-Dirac statistics.

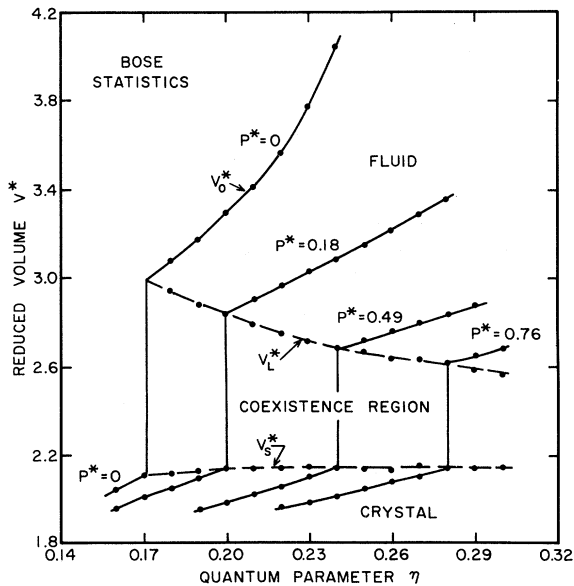


FIG. 7. Same graph as in Fig. 6 but for systems which obey Bose-Einstein statistics.

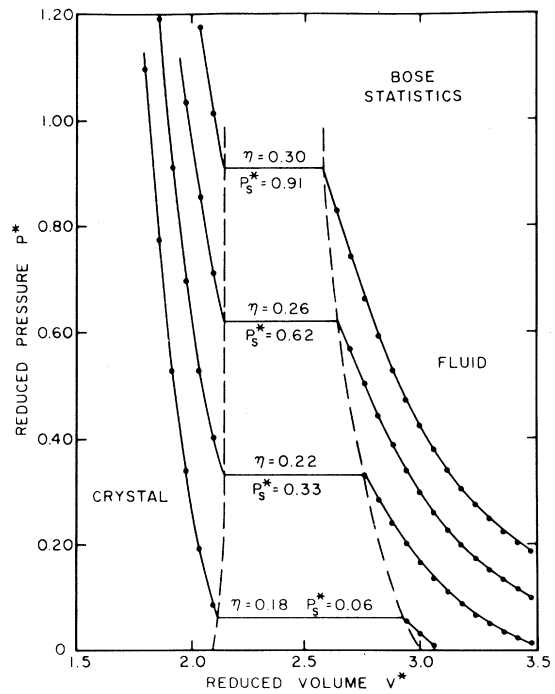


FIG. 9. P^*-V^* diagram with lines of constant η for Lennard-Jones systems at zero temperature with Bose-Einstein statistics.

of T in the usual formulation. One finds

$$\eta_c = 3v_0^*/2V^*(k_F^*)^2. \quad (\text{A7})$$

The value of $\delta = \delta_m$ which minimizes E^* is given by

$$\begin{aligned} \delta_m &= (-A/B)^{1/2}, \quad \eta \leq \eta_c \\ &= 0, \quad \eta \geq \eta_c. \end{aligned} \quad (\text{A8})$$

With (A8) in (A5), we find

$$\begin{aligned} E^* &\cong E_n^*, \quad \eta \geq \eta_c \\ &\cong E_n^* - A^2/4B, \quad \eta \leq \eta_c. \end{aligned} \quad (\text{A9})$$

It is straightforward to show that at $\eta = \eta_c$ φ^* is continuous, but that

$$\lim_{\epsilon \rightarrow 0} \left[\left(\frac{\partial \varphi^*}{\partial \eta} \right)_{\eta_c + \epsilon} - \left(\frac{\partial \varphi^*}{\partial \eta} \right)_{\eta_c - \epsilon} \right] = \left[\frac{1}{2B} \left(\frac{\partial A}{\partial \eta} \right)^2 \right]_{\eta = \eta_c}, \quad (\text{A10})$$

which, since $\partial \varphi^*/\partial \eta = \partial^2 E^*/\partial \eta^2$, indeed demonstrates a second-order transition as η is varied.

APPENDIX B

The numbers collected in Tables II and III were all obtained by Monte Carlo evaluation of the many-body integrals given in Eqs. (4.7) and (4.19) and therefore have some scatter due to statistical

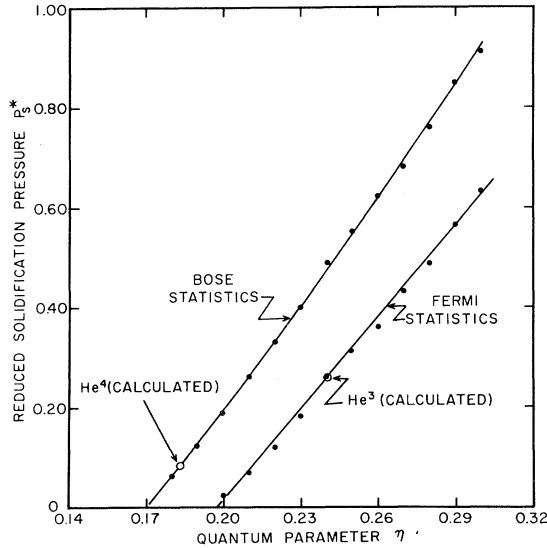


FIG. 10. Dependence of the reduced solidification pressure P_s^* upon the quantum parameter η for Lennard-Jones systems with either Fermi-Dirac or Bose-Einstein statistics. Note that a curve extrapolated through the He^3 and He^4 points, ignoring statistics, would give an incorrect representation of the dependence of P_s upon larger η .

error in the Monte Carlo calculations. In order to minimize the effect of this scatter and also to provide a means of interpolating, it was useful to find a polynomial fit to these data in terms of a convenient set of reduced parameters. The basic scaling equation for the reduced ground-state energy may be written

$$\begin{aligned} E^*(\rho; A, b) &= S^6 F_1(\rho_0; A_0, b_0) + S^{12} F_2(\rho_0; A_0, b_0) \\ &\quad + \eta S^2 F_3(\rho_0; A_0, b_0), \end{aligned} \quad (\text{B1})$$

where S is defined by (4.4) and, by comparison with (4.5), the F_i have the general form

$$F_1(\rho_0; A_0, b_0) = -4 \langle (\sigma/r)^6 \rangle_0, \quad (\text{B2a})$$

$$F_2(\rho_0; A_0, b_0) = 4 \langle (\sigma/r)^{12} \rangle_0, \quad (\text{B2b})$$

$$F_3(\rho_0; A_0, b_0) = \langle t/N \rangle_0. \quad (\text{B2c})$$

The specific forms of the F_i for the Bose fluid, Fermi fluid, and crystalline systems must be determined by comparison with Eqs. (4.10), (4.16), and (4.17), respectively. For a fixed reference density, the dimensionless functions F_i ($i=1, 2, 3$) depend only upon the variational parameters A_0 and b_0 (of course there is no A_0 parameter for the fluid phase). The quantities F_i were fitted by cubic polynomials in the variational parameters and these analytic expressions were used in the scaling equations to determine the value of the variational parameters which minimize the energy at a given density. The reduced pressure curves were also obtained by evaluating the volume derivative of the parametrized scaling equation. Because there is only one variational parameter in our description of the fluid phase, while there are two parameters in the crystalline variational wave function, we have used different forms of cubic polynomials for the two phases.

The $F_i(\rho; A, b)$ for the crystalline phase were fitted by a cubic polynomial of the form

TABLE IV. Values of the coefficients $W_{jk}^i(\rho_0)$ in the two-dimensional cubic polynomial fit to the quantities $F_i(\rho_0; A_0, b_0)$ in the scaling equation (B1) for the crystalline phase. The reference density is $\rho_0 = 0.02803$ atoms/ \AA^3 . The W coefficients are dimensionless.

j	k	W_{jk}^1	W_{jk}^2	W_{jk}^3
0	0	-95.752	263.87	84.949
0	1	2.2847	-9.8520	1.7685
0	2	-0.081912	0.26168	0.014423
0	3	0.0022193	-0.0024319	-0.0052971
1	0	208.50	-585.16	-209.03
1	1	-2.3645	12.863	-2.9053
1	2	0.029354	-0.17192	0.091066
2	0	-164.70	443.40	172.49
2	1	0.64896	-4.2144	0.91878
3	0	44.728	-114.17	-39.957

TABLE V. Cubic-spline-function parameters C_{ij} , g_{ik} , and D_{ik} in the polynomial fit to the quantities $F_i(\rho_0; b_0)$ in the scaling equation (B1) for the Fermi fluid. The reference density is $\rho = 0.01967$ atoms/ \AA^3 . The tabulated parameters are all dimensionless. There are five discontinuities in this spline function.

j	C_{1j}	C_{2j}	C_{3j}	k	g_{1k}	D_{1k}	g_{2k}	D_{2k}	g_{3k}	D_{3k}
0	-34.3105	138.887	38.4306	1	1.144 09	-2.650 87	1.173 89	13.7311	1.126 40	7.489 28
1	69.5774	-323.125	-92.2189	2	1.196 04	-2.529 57	1.201 82	13.6510	1.136 15	7.786 97
2	-52.2032	254.360	74.4860	3	1.206 20	-2.439 58	1.236 74	12.0999	1.157 52	7.814 54
3	13.5248	-67.4185	-16.9336	4	1.223 27	-2.287 87	1.239 59	11.9164	1.191 51	6.694 82
				5	1.298 47	-1.442 94	1.278 22	8.786 28	1.202 51	6.226 96

$$F_i(\rho; A, b) = \sum_{0 \leq j+k=3} W_{jk}^i(\rho) (b^*)^j (A^*)^k, \quad (\text{B3})$$

where $b^* \equiv b/\sigma$, $A^* \equiv A\sigma^2$, and the coefficients $W_{jk}^i(\rho)$ were determined by a least-squares fit to the crystalline $F_i(\rho_0; A_0, b_0)$ evaluated from Table III at the reference density $\rho_0 = 0.02803$ atoms/ \AA^3 . The $W_{jk}^i(\rho_0)$ coefficients are presented in Table IV.

In the fluid phase the F_i depended upon only one variational parameter. It was therefore convenient to use the more flexible cubic spline functions rather than simple cubic polynomials. The spline function is of the form

$$F_i(\rho; b) = \sum_{j=0}^3 C_{ij} (b^*)^j + \sum_{k=1}^{N_i} \Theta(b^* - g_{ik}) D_{ik} (b^* - g_{ik})^3, \quad (\text{B4})$$

where $\Theta(x)$ is a Heaviside function defined by

$$\begin{aligned} \Theta(x) &\equiv 0, & x < 0 \\ &\equiv 1, & x \geq 0. \end{aligned} \quad (\text{B5})$$

The spline function, (B4), is characterized by its third derivative having discontinuities of magnitude D_{ik} at the N_i points g_{ik} .

For the Fermi fluid the best fit was obtained using five discontinuities. The parameters C_{ij} , D_{ik} , and g_{ik} were determined by a least-squares fit to the Fermi fluid $F_i(\rho_0; b_0)$ evaluated at the reference density $\rho_0 = 0.01967$ atoms/ \AA^3 using those b_0 values in Table II for which the exchange energies are also entered. The spline parameters for the Fermi fluid are collected in Table V.

For the Bose fluid the best fit was obtained by separating the range of b values into two intervals and fitting each interval separately with one discontinuity in each interval. The two sets of parameters C_{ij} , D_{ik} , and g_{ik} were determined by a least-squares fit to the Bose fluid $F_i(\rho_0; b_0)$ evaluated at the reference density $\rho_0 = 0.01967$ atoms/ \AA^3 using all b_0 values in Table II. The spline parameters for the Bose fluid are presented in Table VI for the two intervals $0.988 < b^* < 1.222$ and $1.222 < b^* < 1.450$.

TABLE VI. Two sets of cubic-spline-function parameters C_{ij} , g_{ij} , D_{ij} for the polynomial fit to the quantities $F_j(\rho_0; b_0)$ in the scaling equation (B1) for the Bose fluid. The parameters are presented for one discontinuity in each of the two intervals: interval I, $0.988 < b^* < 1.222$, interval II, $1.222 < b^* < 1.450$. The tabulated parameters are dimensionless.

Interval	i	C_{i0}	C_{i1}	C_{i2}	C_{i3}	g_{i1}	D_{i1}
I	1	-36.1229	70.2092	-50.8085	12.7993	1.127 20	-0.432 945
	2	183.395	-427.263	336.629	-89.2978	1.113 34	0.930 576
	3	46.6451	-118.809	101.417	-25.0240	1.104 30	1.708 08
II	1	-30.5998	53.7714	-34.9550	7.809 15	1.340 03	0.055 476
	2	54.8221	-108.057	72.4583	-16.4222	1.298 22	0.112 695
	3	-41.3211	110.259	-97.1528	32.2740	1.330 74	-0.205 403

*Work partially supported by a grant from the Research Corporation, by the Atomic Energy Commission under Contract Nos. AT(11-1)1569 and AT(11-1)1764, and by a grant from the National Science Foundation.

¹J. de Boer, *Physica* **14**, 139 (1948).

²J. de Boer and B. S. Blaisse, *Physica* **14**, 149 (1948).

³J. de Boer and R. J. Lunbeck, *Physica* **14**, 520 (1948).

⁴See, e.g., J. O. Hirschfelder, C. F. Curtiss, and R. B. Bird, *Molecular Theory of Gases and Liquids* (Wiley, New York, 1954), p. 244.

⁵P. W. Anderson and R. G. Palmer, *Nature Phys. Sci.* **231**, 145 (1971); *Phys. Rev. D* **9**, 3281 (1974).

- ⁶J. W. Clark and N. C. Chao, *Nat. Phys. Sci.* 236, 37 (1972); J. W. Clark, in *Proceedings of the Symposium on Present Developments in the Many-Body Problem, Rome, 1972* (to be published); N. C. Chao, thesis (Washington University, St. Louis, Mo., 1973) (unpublished).
- ⁷B. Banerjee, S. M. Chitre, and V. K. Garde, *Phys. Rev. Lett.* 25, 1125 (1970).
- ⁸R. L. Coldwell, thesis (University of Washington, Seattle, 1969) (unpublished); R. L. Coldwell, *Phys. Rev. D* 5, 1273 (1972).
- ⁹V. Canuto and S. M. Chitre, *Phys. Rev. Lett.* 30, 999 (1973); *Nat. Phys. Sci.* 243, 63 (1973).
- ¹⁰V. R. Pandharipande, *Nucl. Phys. A* 217, 1 (1973).
- ¹¹L. H. Nosanow and L. J. Parish, *Ann. N. Y. Acad. Sci.* 224, 226 (1973).
- ¹²V. Canuto and S. M. Chitre, *Phys. Rev. D* 9, 1587 (1974).
- ¹³D. Schiff, *Nat. Phys. Sci.* 243, 130 (1973).
- ¹⁴S. Cochran and G. V. Chester (unpublished).
- ¹⁵E. Østgaard, *Phys. Lett. B* 47, 303 (1973).
- ¹⁶S. Chakravarty, M. D. Miller, and C.-W. Woo, *Nucl. Phys. A* 220, 223 (1974).
- ¹⁷R. P. Feynman, *Phys. Rev.* 56, 340 (1939); H. Hellmann, *Einführung in die Quantenchemie* (Deuticke, Leipzig, 1937).
- ¹⁸W. L. McMillan, *Phys. Rev.* 138, A442 (1965).
- ¹⁹D. Schiff and L. Verlet, *Phys. Rev.* 160, 208 (1967).
- ²⁰J. P. Hansen and D. Levesque, *Phys. Rev.* 165, 293 (1968).
- ²¹J. P. Hansen and E. L. Pollock, *Phys. Rev. A* 5, 2651 (1972).
- ²²F. Y. Wu and E. Feenberg, *Phys. Rev.* 122, 739 (1961).